

# Maximize Your Diffusion: A Study into Reward Maximization and Alignment for Diffusion-based Control.

Dom Huh<sup>1</sup> Prasant Mohapatra<sup>1,2</sup>

## Abstract

Diffusion-based planning, learning, and control methods present a promising branch of powerful and expressive decision-making solutions. Given the growing interest, such methods have undergone numerous refinements over the past years. However, despite these advancements, existing methods are limited in their investigations regarding general methods for reward maximization within the decision-making process. In this work, we study extensions of fine-tuning approaches for control applications. Specifically, we explore extensions and various design choices for four fine-tuning approaches: reward alignment through reinforcement learning, direct preference optimization, supervised fine-tuning, and cascading diffusion. We optimize their usage to merge these independent efforts into one unified paradigm. We show the utility of such propositions in offline RL settings and demonstrate empirical improvements over a rich array of control tasks.

## 1. Introduction

Denosing diffusion probabilistic models (DDPM) have demonstrated incredible successes in numerous domains as one of the de facto standards for generative modeling in continuous domains (Sohl-Dickstein et al., 2015; Ho et al., 2020; Yang et al., 2024), garnering heightened attention in research communities with the model’s exceptional ability to capture highly complex data distributions and flexibility in constraint-based optimization that can be applied to diverse modalities. A notable direction is their adoption and realizations in decision-making applications (Zhu et al., 2024), contributing to an evolving class of model-based planning as well as model-free algorithms we will refer to as diffusion-based planning, learning, and control. Despite the appealing promises of DDPMs, the algorithm’s sample

<sup>1</sup>Department of Computer Science, University of California, Davis, USA <sup>2</sup>University of South Florida, USA. Correspondence to: Dom Huh <dhuu@ucdavis.edu>.

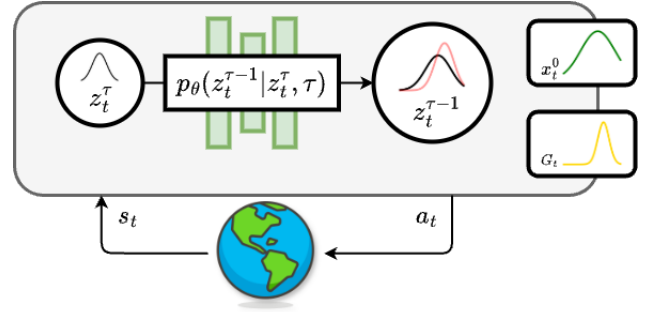


Figure 1: A illustration of the reward maximization of diffusion model for control, visualizing the diffusion process at  $\tau \rightarrow \tau - 1$  such that  $z_t^{\tau-1}$  is denoised towards the target distribution  $x_t^0$  but also aligned with maximize the return distribution  $G_t$ , shown in red.

generation inefficiencies loom as a notorious and significant concern (Cao et al., 2024), causing a severe bottleneck as an efficient solution for closed-loop control.

The focus of this work addresses this limitation, proposing a general investigation into reward maximization, or more aptly called *reward alignment*, directly on the diffusion process for control. In turn, our objective is to reduce the *number of samples* required to generate to maximize the reward signal. We adopt modern optimization procedures to facilitate a guided and constrained distributional shift biased towards maximal returns. Specifically, we investigate four reward alignment approaches — reward maximization with reinforcement learning, direct preference optimization, supervised fine-tuning, and cascading diffusion — and compare their performance in various control settings, more so in offline RL settings. We evaluate various design choices as well as an unification of the studied alignment approaches on a diverse testbed of challenging control tasks consisting of a variety of complex tasks from benchmarks such as D4RL (Fu et al., 2020), MetaWorld (Yu et al., 2021), PushT (Florence et al., 2022), Relay-Kitchen (Gupta et al., 2019), and RoboMimic (Mandlekar et al., 2021) as well as a novel evaluation task that enables in-depth analysis and visualization of the various features of the environment, the controller and their interactions.

## 2. Background

**Diffusion Models** DDPMs (Ho et al., 2020) are commonly known as a class of generative models, which aim to estimate and sample from unknown data distributions  $X$ . DDPMs define a Markov chain of forward Gaussian kernels  $q(x_t|x_{t-1})$  with a scheduled (Nichol & Dhariwal, 2021) sequence of variance coefficients  $\{\beta_t \in (0, 1)\}_{t=1}^T$  that gradually add noise to input data

$$q(x_t|x_{t-1}) = \mathcal{N}(x_t; \sqrt{1 - \beta_t}x_{t-1}, \beta_t \mathbf{I}) \quad (1)$$

and then learn to reverse the diffusion process by denoising with learnable reverse Gaussian kernels  $p_\theta(z_{t-1}|z_t)$ , parameterized by  $\theta$ , to generate data samples  $z_0$  from a standard Gaussian noise prior  $z_T \sim \mathcal{N}(0, \mathbf{I})$ .

$$p_\theta(z_{t-1}|z_t) = \mathcal{N}(z_{t-1}; \mu_\theta(z_t, t), \Sigma(z_t, t)) \quad (2)$$

A common practice is to parameterize  $\mu_\theta(z_t, t)$  to perform  $\epsilon$ -prediction, motivated by its resemblance to the Langevin dynamics, which enables a simplification of the training objective.

$$\mu_\theta(z_t, t) := \frac{1}{\sqrt{\alpha_t}} \left( z_t - \frac{1 - \alpha_t}{\sqrt{1 - \bar{\alpha}_t}} \epsilon_\theta(z_t, t) \right) \quad (3)$$

The training objective of DDPM uses the variational lower bounds of the marginal likelihood to minimize the negative log-likelihood (Kingma et al., 2021), as shown in Equation 4, where in practice, a simplified yet equivalent objective  $\mathcal{L}_{\text{DDPM}}(\theta)$  is commonly used (Ho et al., 2020).

$$\mathcal{L}_{\text{NLL}}(\theta) = \mathbb{E}[-\log p_\theta(z_0)] \leq -\mathbb{E}_q[\log \frac{p_\theta(z_{0:T})}{q(x_{1:T}|x_0)}] \quad (4)$$

$$\mathcal{L}_{\text{DDPM}}(\theta) = \mathbb{E}_{x_0} \left[ \|\epsilon_t - \epsilon_\theta(\sqrt{\bar{\alpha}_t}x_0 + \sqrt{1 - \bar{\alpha}_t}\epsilon_t, t)\|^2 \right] \quad (5)$$

where  $t \sim [0, T]$  with  $T$  is the total number of diffusion steps,  $\beta_t = 1 - \alpha_t$ ,  $\bar{\alpha}_t = \prod_{i=1}^t \alpha_i$ , and  $\epsilon_t \sim \mathcal{N}(0, \mathbf{I})$ . A common and useful intuition is that DDPMs learn information regarding a time-dependent vector field  $u_t(z_t, \theta)$  that generates a probability density/diffusion path  $p_t(z_{t-1}|z_t)$  from a simple and known distribution (e.g., standard Gaussian) to the unknown target distribution (e.g., data distribution).

Several recent improvements and reformulations of this DDPM paradigm have been explored (Cao et al., 2024), most notably and relevantly, towards efficient sample generation with implicit probabilistic models (DDIM (Song et al., 2020a)),  $v$ -prediction (Salimans & Ho, 2022) and rectification (Liu et al., 2022; Wang et al., 2024), conditional guidance (Dhariwal & Nichol, 2021; Ho & Salimans, 2022), model selection (Rombach et al., 2022; Ho et al., 2022; Peebles & Xie, 2023), novel DDPM training paradigms (Fan & Lee, 2023; Black et al., 2023) and related classes of generative modeling such as score/flow-matching (Song et al., 2020b; Lipman et al., 2023).

**Alignment of Diffusion Paths** Training deep learning models, such as a DDPM, is often done in two stages. In the first stage, the foundation model is optimized, where a general underlying data distribution is learned by training on large-scale datasets. In the second stage, this foundation model is fine-tuned to align to a reference distribution (e.g., towards downstream tasks, human preference, or stitching with multiple distributions) through supervised fine-tuning (SFT) (Ziegler et al., 2019), RL with AI/human feedback (RLAIF/RLHF) (Bai et al., 2022; Ouyang et al., 2022a), preference optimization (DPO) (Rafailov et al., 2024; Wallace et al., 2024; Xiao et al., 2024), or reward gradients (Prabhudesai et al., 2023; Clark et al., 2023). In this work, we apply and modify these techniques toward DMCs to better align using a scalar feedback signal that defines the reward distribution for sequential decision-making tasks.

**Diffusion Models for Control (DMC)** Like many generative modeling algorithms, the role of DDPMs in decision-making applications has spanned from diffusion-based planning (Janner et al., 2022) to policy learning (Ren et al., 2024), with significant successes and advancements in online and more prevalently in offline RL settings. Specifically, its utilization has been quite diverse, taking various forms such as diffusion-based policies, value functions, and world models, and these models can either indirectly support the training of RL policies (Rigter et al., 2023) or be more of an active component of the decision-making loop (Wang et al., 2022; Chen et al., 2022). In this work, we extend these prior efforts, specifically Diffuser (Janner et al., 2022), Diffusion Policy (DP) (Chi et al., 2023), SynthER (Lu et al., 2024) and some of their following works (Ajay et al., 2023; Dong et al., 2024a) to act as our foundation to build upon with our alignment efforts.

## 3. Reward Alignment of DMC

We define a general equation that defines the reward alignment optimization problem, in which we align our diffusion model  $\pi_\theta$  to generate samples  $z_0$  that maximize a reward function.

$$\mathcal{L}_{\text{align}}(\theta) := \underbrace{\mathbb{E}_{z_0 \sim \pi_\theta} [r(z_0)]}_{\text{Reward Maximization}} \text{ s.t. } \underbrace{\text{div}(\pi_\theta, X)}_{\text{Divergence Constraint}} \leq \delta \quad (6)$$

The constraint subjects the optimization to ensure the generated samples remain within a plausible region of the target data distribution  $X$ , or the distribution learned by the foundation DDPM  $\pi_{\text{fdt}}$ .

We illustrate this objective in Figure 2, where a foundation DDPM is fine-tuned to maximize a given reward function on a toy task. In this example, the fine-tuned diffusion paths largely adhere to the foundation model, with minor yet impactful adjustments towards maximizing their respective

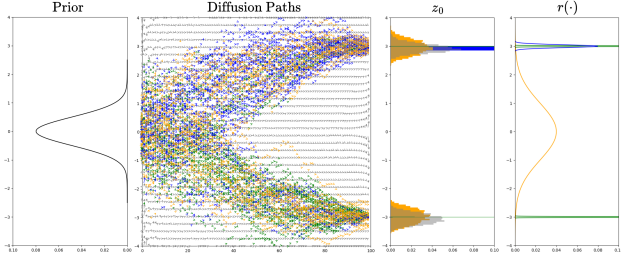


Figure 2: A visualization of the effects of alignment to the diffusion process. Given a foundation DDPM, whose outputs and diffusion field over the entire state space are shown in gray, we align its diffusion process to maximize three separate reward functions, shown in orange, green and blue.

reward functions, exceeding  $\times 3.21$ ,  $\times 7.09$ , and  $\times 4.18$  improvements in orange, green and blue respectively within 32 generated samples while maintaining  $\Pr(z_0|X) \gg 0$ . Specifically, with the orange reward function, despite having the potential to converge towards out-of-distribution (OOD) regions for maximal rewards, the constraints are in place to adequately address this issue in a desired manner. Hence, to achieve this alignment, we study and extend four approaches – RL, DPO, SFT, and cascading – to optimize the objective in Equation 6.

An important distinction between DDPM and DMC is that, at denoising step  $t$ , DMC specifies that  $z_t$  is either a  $N$ -step state-action trajectory  $\{s_0, a_0, s_1 \dots s_N\}^t$  (e.g. Diffuser and DD), or actions  $a_t^t$ , (e.g. DP) with a conditional information regarding the state  $s_t$ , as shown in Figure 3. Hence, our reward function  $r(z_0)$  can either represent the return of the state-action trajectory or the Q-value of each state-action pair for greater granularity as a way to take advantage of the temporal aspect of the latent representation.

### 3.1. Reward Alignment with Reinforcement Learning

A natural approach to reward maximization is to extend traditional RL optimization to align the denoising process towards sample generation with higher returns. To do so, we view the DMC as a denoising policy

$$\pi_\theta(\mu_t|z_t, c) = p_\theta(z_t|z_{t-1}, c) \quad (7)$$

with a condition input  $c$ , treating the denoising process as a multi-step MDP (Black et al., 2023). We build upon two classic RL algorithms that directly optimize Equation 6: REINFORCE (Williams, 1992) and Q-value policy gradient (QV-PG) (Silver et al., 2014; Haarnoja et al., 2018).

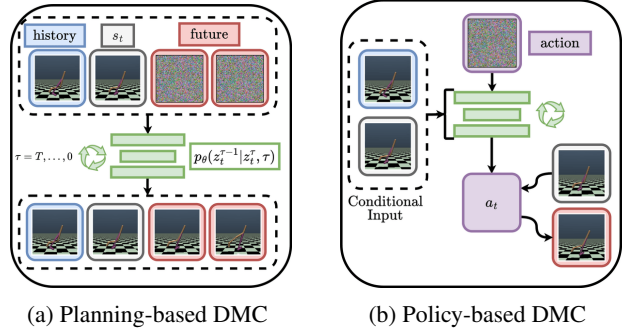


Figure 3: A visual illustration of the two DMC frameworks on Walker2D task, where the planning-based DMC is forecasting future states and the policy-based DMC generates actions directly.

$$\mathcal{L}_{\text{REINFORCE}}(\theta) = \mathbb{E}\left[\sum_{t=0}^T \kappa_t \text{sg}(\log \pi_\theta(\mu_t|z_t), K) r(z_0)\right] \quad (8)$$

$$\mathcal{L}_{\text{QV-PG}}(\theta) = \mathbb{E}[\kappa_t r(\text{sg}(\pi_\theta(\mu_{0:T}|z_{0:T}), K))] \quad (9)$$

To account for the sequential nature of the denoising process, we consider two important training concerns: gradient truncation and denoising credit assignment.

- Gradient truncation clips the gradient such its calculation only propagates through the last  $K$  steps (Clark et al., 2023; Prabhudesai et al., 2023), where  $K$  can be dynamically set during training. This truncation implements truncated backpropagation through time/denoising steps, facilitating a more memory-efficient and stable optimization. In practice, we utilize the stop-gradient function  $\text{sg}(\cdot, K)$ , which truncates the gradient computation to the last  $K$  denoising steps.
- As each sampling step contributed differently towards reaching  $z_0$ , we consider the concept of credit assignment over the denoising steps. Empirically, we define a sequence of hyperparameters  $\{\kappa_0, \kappa_1, \dots\}$  that scale the objective along the denoising steps. In this work, we consider two options, where  $\kappa$  can be a decreasing sequence or  $\kappa_t$  can be the similarity measure between  $(z_t, z_{t-1})$  and  $(z_T, z_0)$ , a computation that is done retrospectively.

To prevent large divergence from the reference policy/foundation DMC and adhere to the constraint in Equation 6, we can use trust regions with clipping, i.e., proximal policy optimization (PPO) (Schulman et al., 2017), similar to the procedure introduced with DDPO (Black et al., 2023), or add a KL regularization term. We found both REINFORCE/PPO and QV-PG approaches to be competitive,

to which their comparison seems moot, and the one that performed better is kept during evaluation.

### 3.2. Reward Alignment with Preference Optimization

Direct preference optimization (DPO) (Rafailov et al., 2024) offers an alternative approach to align DMC by utilizing a dataset of ranked pairs  $x_0^l \prec x_0^w$  of losing and winning samples and maximizing the likelihoods of the DMC’s sample generation following the preference operator  $\prec$ . This preference operation is defined in this work as follows:

$$x_0^l \prec x_0^w \implies \mathbb{E}[r(x_0^l)] < \mathbb{E}[r(x_0^w)] \quad (10)$$

Following DiffusionDPO adaptation (Wallace et al., 2024), the DPO objective  $\mathcal{L}_{\text{DPO}}(\theta)$  is simplified and can be expressed as follows:

$$\mathcal{L}_{\text{DPO}}(\theta) = -\mathbb{E}[\log \sigma(-\gamma\omega(\lambda_t)(F_w(\theta) - F_l(\theta)))] \quad (11)$$

where  $\sigma(\cdot)$  is the sigmoid function,  $\lambda = \alpha_t^2/\sigma_t^2$  is the signal-to-noise ratio,  $\omega(\lambda_t)$  is a weighting function and

$$F_*(\theta) = \|\epsilon^* - \epsilon_\theta(z_t^*, t)\|_2^2 - \|\epsilon^* - \epsilon_{\text{ref}}(z_t^*, t)\|_2^2 \quad (12)$$

A functional representation of the preference operator can be expressed either heuristically or, more generally, as a trajectory-wise value function (Zhang et al., 2024).

### 3.3. Reward Alignment with Supervised Fine-Tuning

Similar to DPO, we can instead fine-tune the foundation DMC only using the winning samples, or samples with the highest rewards, by updating along  $\mathcal{L}_{\text{DDPM}}(\theta)$  on these samples. Therefore, we apply traditional diffusion updates to shift and concentrate the generative distribution towards higher rewards under a stable optimization scheme, i.e., supervised learning.

This process can be performed iteratively, using either the foundation or the fine-tuned DMC as a data synthesizer to generate samples of increasingly higher returns. However, if we use the fine-tuned DMC, we face potential instability and OOD issues. In this work, we prevent this using a threshold constraint that prevents samples with lower likelihoods of the foundation DMC from being used for an SFT update.

### 3.4. Up-sampling Reward with Cascading Diffusion

Cascading DDPM (Ho et al., 2022) is an up-sampling technique used for super-resolution, where lower resolution samples are processed as the conditional inputs to sample higher resolution samples. This concept can be extended to control applications, where a DMC that is conditioned on  $x_0^{\text{cond}}$  is trained to generate a sample  $x_0^r$  that yields greater rewards, hence  $r(x_0^{\text{cond}}) < r(x_0^r)$ .

In prior efforts with similar motivations (Zhang et al., 2024), the objective followed classifier-free guidance (CFG), training with the conditional information at some probability  $p \in [0, 1]$ . Since, in our case, the cascading DMC is connected to a foundation DMC, it does not necessarily have to emphasize the generation of the target distribution; we set  $p = 1$ . Transferring the trained weights from a foundation DMC as a warm-start proved beneficial and was likely sufficient to understand the target distribution.

An important consideration for training cascading DMC is determining the pairs  $(x_0^{\text{cond}}, x_0^r)$  of samples to condition and reference during training, where their alignment may be mismatched, especially for multi-step samples. To address this, when curating  $(x_0^{\text{cond}}, x_0^r)$ , we promote consistency between the pairs. This consistency can be achieved by in-painting a contiguous subset of the sample or sharing the latent state  $z_t$  at a denoising step  $t$ . These approaches force some level of relations between the two samples, such that the cascading DMC avoids up-sampling towards random samples during inference.

To further boost the up-sampling capability of the cascading DMC, we can extend the other alignment approaches to greaten the difference between  $r(x_0^{\text{cond}})$ ,  $r(x_0^r)$  with proper modifications. Our exploration of this study is limited, and we encourage future works to research this topic further.

### 3.5. An Unification of Reward Alignment Approaches

The four alignment methods discussed above—RL, DPO, SFT, and cascading—share a unified goal of solving the constrained optimization problem defined by Equation 6. While each approach is suited for different use cases, with their unique advantages and limitations, we find that they can be applied together. As the cost of increasing model alignment efforts is modest relative to training the reference policy (Ouyang et al., 2022b), we propose a sequential optimization scheme, where each alignment approach (i.e., RL, DPO, and SFT) is used individually, and repeatedly until convergence. This iterative sequential scheme is practiced to avoid potential catastrophic learning variances of a naive multi-objective optimization approach. We find that after 2–3 passes of this sequence, there are diminishing returns in the reward maximization efforts. Again, the cascading module is trained separately and appended onto the fine-tuned model during inference. Similarly, we experimented with performing multiple passes through the cascading module but found high variances in the up-sampling after 2 passes.

### 3.6. Design and Training Choices

**Diffusion Sampling and Process** We apply the proposed alignment methods to widespread advancements to the classical DDPM formulation. For instance, accelerated sampling methods such as DDIM (Ho et al., 2020) and other

Table 1: A Summary of Alignment Method Comparison: Reward terms and divergence control mechanisms.

Method	Reward Maximization Term	Divergence Control
RL	Policy gradient (Eqs. 8, 9)	KL regularization/PPO clipping
DPO	Preference ranking via $F_w - F_l$	Regularization via $\epsilon_{\text{ref}}$
SFT	Fine-tuning on high reward samples	Likelihood threshold using $\pi_{\text{ref}}$
Cascading	Conditional generation $p(x_0^T   x_0^c)$	Warm-starting + adherence to reference policy.

representations of the iterative diffusion-like posterior, such as score-matching (SM) (Song et al., 2020a) and flow-matching (FM) (Lipman et al., 2023), are also studied in this work under the Diffuser, DD and DP framework utilizing these alignment approaches.

**In-painting** The in-painting ability of DDPMs refers to reconstructing missing regions within the data based on the context provided. In our alignment efforts, we rely on this capability to bootstrap training samples to enforce consistency and avoid undesired changes to the sample. To ensure that our model can in-paint effectively, we trained the foundation DMC directly on the in-painting task, where we utilize causal masks along the temporal axis following the Repaint procedure for conditioning (Lugmayr et al., 2022). This in-painting procedure is followed during inference for planning-based DMC. In our experiments, we found that including this masked training improved not only the DMC’s ability to in-paint but also the overall performance of the DMC.

**Context Window and Recurrence** The context window for the DMC defines the number of time steps contained in input for planners and conditional input for the policy. Under specific model architectures, such as a temporal convolution backbone, this window does not face significant computing constraints. However, we opt for a sliding window approach to handle this constraint for backbones that scale poorly along this dimension and for tasks with longer time horizons. We found the introduction of a recurrent state appended to the latent state to cause instability in some of the tasks, and even in certain tasks with less complex observations with greater partial observability, we found minor but negligible improvements.

**Evaluation Function** For all alignment methods, we use a separate Q-value function trained under implicit Q-learning in an offline RL fashion to evaluate the samples generated and calculate the learning signal. The Q-value can also be used during action-selection.

**Online Fine-tuning** We additionally study the inclusion of online fine-tuning, where we inject samples from online interactions during the alignment training to compare and

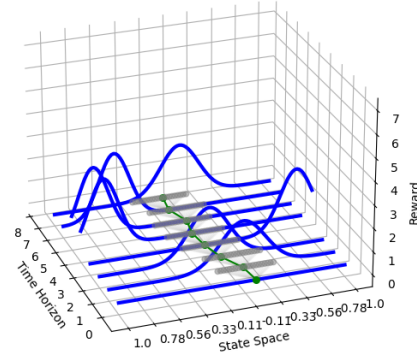


Figure 4: Visualization of the Nav1D task and an example of an agent’s trajectory, shown in green, and the actions space is shown in gray. The reward distributions at every time step are shown in blue.

analyze the changes in performance.

**PEFT** For all alignment processes, we use LORA (Hu et al., 2021), a parameter-efficient fine-tuning approach that introduces a separate set of low-rank weights on linear layers that are trained during fine-tuning. Separate LORA weights were not introduced between different alignment methods.

## 4. Experiments

### 4.1. Tasks

We evaluate our alignment approaches on various offline RL benchmarks. We use D4RL and MetaWorld for planning-based DMC; for policy-based DMC, we use Robomimic, Relay-Kitchen, and PushT. There is a standardized and publicly available offline RL dataset for many of these tasks, and we direct readers toward their respective original works for more details.

**Nav1D** We also introduce simple 1D navigation (Nav1D) task to our testbed, shown in Figure 4, where the agent start at a random position  $s_t \in [-1, 1]$  and must move left or right. The agent must select actions under a continuous yet restricted action space with a deterministic transition dynamics

$$\mathcal{T}(s_t, a_t) = \mathbb{I}(\text{clip}(s_t + \gamma a_t, -1, 1)) \quad (13)$$

Table 2: **Evaluation Results of Planning-based DMC.** The performance of various sampling approaches for planning-based DMC. Results correspond to the average return over 64 episode seeds with 16 roll-outs per action step, where the arrow indicates the results after our proposed alignment fine-tuning process.

Dataset	Environment	Diffuser				DD
		DDPM	DDIM	SM	FM	DDPM
Random	HalfCheetah	8.0 → 12.7	5.5 → 11.3	5.4 → 11.5	10.2 → 15.9	8.4 → 13.5
	Hopper	0.5 → 4.2	0.4 → 1.1	0.2 → 3.0	0.3 → 3.9	0.5 → 1.8
	Walker2d	3.2 → 9.1	4.4 → 10.1	3.6 → 5.9	3.4 → 7.2	3.1 → 6.9
Medium-Expert	HalfCheetah	85.2 → 97.8	77.8 → 94.1	74.3 → 94.3	90.0 → 102.1	86.2 → 93.5
	Hopper	52.5 → 107.2	50.2 → 100.1	66.2 → 111.2	54.8 → 113.2	53.1 → 110.9
	Walker2d	76.5 → 102.4	48.4 → 108.3	65.1 → 109.0	49.1 → 99.4	67.1 → 101.1
Medium	HalfCheetah	30.6 → 48.3	23.3 → 50.6	32.1 → 54.2	35.1 → 50.2	29.0 → 44.5
	Hopper	52.9 → 89.5	61.2 → 93.5	49.0 → 82.0	44.2 → 96.3	37.5 → 90.2
	Walker2d	35.3 → 76.6	29.6 → 61.8	36.1 → 78.0	33.4 → 89.2	29.1 → 50.4
Medium-Replay	HalfCheetah	28.6 → 36.4	22.9 → 34.1	14.1 → 26.5	26.8 → 37.9	25.7 → 36.4
	Hopper	54.1 → 91.8	49.2 → 94.8	55.3 → 77.9	58.5 → 89.4	45.8 → 70.5
	Walker2d	26.0 → 58.6	45.6 → 67.5	46.2 → 59.1	50.5 → 62.7	41.1 → 52.4
Mixed Partial	Franka-Kitchen	41.5 → 56.5	52.0 → 55.9	32.5 → 54.2	45.7 → 52.0	44.5 → 60.3
	Franka-Kitchen	38.0 → 40.1	33.5 → 34.2	36.1 → 41.2	36.3 → 50.1	32.7 → 44.9
Play	Antmaze-Medium	0.2 → 46.7	0.0 → 45.3	0.9 → 84.0	3.2 → 80.8	0.0 → 32.1
	Antmaze-Large	0.0 → 57.3	0.0 → 60.2	3.5 → 76.1	0.7 → 54.9	0.0 → 85.1
Diverse	Antmaze-Medium	0.8 → 42.0	4.0 → 75.3	10.1 → 62.3	11.2 → 92.5	2.4 → 63.2
	Antmaze-Large	0.0 → 47.3	0.0 → 50.6	8.9 → 50.3	0.0 → 70.1	0.8 → 41.3
MetaWorld	Button-Press	0.0 → 0.7	0.1 → 1.0	0.0 → 0.5	0.0 → 0.7	0.1 → 0.5
	Drawer-Open	0.2 → 0.9	0.1 → 0.9	0.2 → 0.7	0.4 → 0.6	0.3 → 0.9
	Sweep-Into	0.3 → 0.7	0.0 → 0.8	0.5 → 0.8	0.3 → 0.9	0.2 → 1.0
	Plate-Slide	0.2 → 0.6	0.1 → 0.4	0.2 → 0.7	0.4 → 0.7	0.1 → 0.6
Nav1D	Partial	2.1 → 4.3	1.9 → 3.3	2.5 → 4.1	2.3 → 5.2	2.0 → 3.9
	Full	3.2 → 6.9	4.3 → 7.3	2.9 → 6.9	3.9 → 6.8	3.3 → 6.9
	Expert	6.2 → 7.3	5.9 → 7.2	5.9 → 7.2	6.4 → 7.1	6.2 → 7.2

where  $\gamma$  is the step size. The objective is to maximize the rewards defined by a sequence of independent normal distribution  $\{N_t\}_{t=0}^H$ , where

$$r(s_t, a_t) \propto \Pr(T(s_t, a_t) = N_{t+1}) \quad (14)$$

over a fixed time horizon  $H$ . The reward distributions are independent from one another and stationary upon repeated trials. The agent’s observation space consists of its current location and additional information that gives the agent a better time-dependent context.

We create three datasets for Nav1D that provide varying state coverages—partial, full, and expert—where both partial and full datasets follow a random policy, and the expert dataset contains trajectories that follow an expert policy.

**Coherency Score** We introduce a coherency score  $C$  to evaluate the sample quality of planning-based DMC,

$$C = \mathbb{E}_{(s_t, a_t, s_{t+1}) \sim \pi_\theta} [\Pr(s_{t+1} = \mathcal{T}(s_t, a_t))] \quad (15)$$

and of policy-based solutions,

$$C = \mathbb{E}_{a_t \sim \pi_\theta} [\Pr(a_t = \pi_\beta(a_t | s_t))] \quad (16)$$

The coherency score measures how well the planning methods capture the dynamics model distribution, whereas, for the policy-based DMC, it measures how well the DMC models the behavior policy  $\pi_\beta$ .

## 4.2. Implementation Details

The basis of our implementation is built upon CleanDiffuser (Dong et al., 2024b), with adjustments made for the alignment methods. A central difference in our implementation of the DMC is the lack of a return conditional input, as it is generally unknown what return is desired. Hence, for action selection, we use the learned Q-Value function to greedily select actions, similar to IDQL (Hansen-Estruch et al., 2023). For DP, we also experiment with expectation-based action selection, where the average over all generated action samples is taken. The model architecture for each algorithm we studied follows the original work, similar to CleanDiffuser. All experiments presented were executed on 3 Nvidia RTX A6000 and Intel Xeon Silver 4214R @ 2.4GHz.

## 4.3. Results For Planning-based DMC

We summarize our finding for planning-based DMC in Table 2, showing the notable improvements from our proposed alignment process, regardless of the sampling approaches such as DDPM, DDIM, SM, FM, and DD frameworks, with decision-making that uses a small number of roll-outs during its planning. Specifically, for each task and algorithm, we first trained the reference DMC and finetuned it using varying passes and iterations through {RL, DPO, SFT} alignments.

We closely examined the learning for these training to ensure no training collapses occurred, with model check-pointing

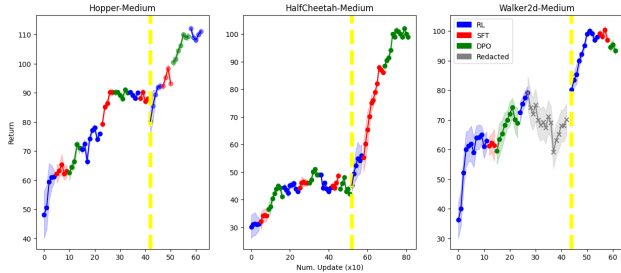


Figure 5: Alignment Learning Curve for Diffuser (DDPM) on the D4RL Medium Datasets, where the average and  $\pm 1$  standard deviation is shown over 64 episode seeds. The yellow vertical line indicates when the online fine-tuning is introduced.

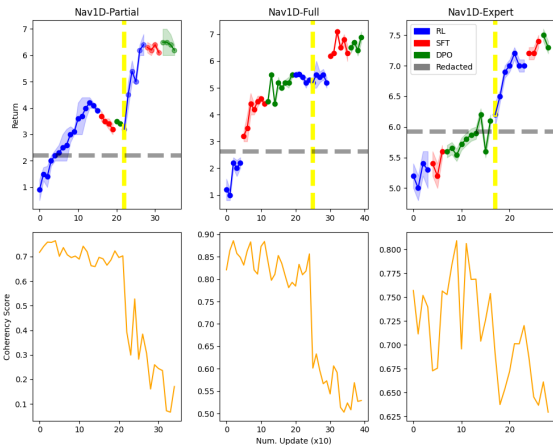


Figure 6: Alignment Learning Curve and Coherency Score for DP (Expectation) on the Nav1D Datasets, where the average and  $\pm 1$  standard deviation is shown over 32 episode seeds. The yellow vertical line indicates when the online fine-tuning is introduced and the black horizontal line represents the average return achieved in the respective dataset.

and lowered learning rates. This phenomenon includes sudden drops in return and instabilities/spikes in the training objectives. We did observe some instances of this, especially during the RL finetuning, which we redacted. We trained the cascading DDPM separately, applying the same alignment process, and attached it for the final evaluation. In general, we found that even with multiple rounds, the return did improve, as shown in Figure 5.

An important trend we noticed as a result of the alignment is that, on average, over all tasks and algorithms, the average standard deviation over the return on all trials significantly decreased, from 38.1%  $\rightarrow$  5.3%. This result empirically indicates the distributional shift that occurs, which narrows the diffusion process towards higher returns, as the average return improved by +43.0%. Using only the D4RL tasks,

Table 3: **Evaluation Results of Policy-based DMC.** The performance of two action-selection methods (expectation vs IDQL policy extraction) for policy-based DMC. Results correspond to the average return over 16 episode seeds on 8 action candidates, where the arrow indicates the results after our proposed alignment fine-tuning process.

Dataset	Environment	DP	
		Expectation	IDQL
Low-Dim	pusht	0.42 $\rightarrow$ 1.0	0.71 $\rightarrow$ 1.0
	relay-kitchen	0.75 $\rightarrow$ 1.0	0.98 $\rightarrow$ 1.0
	lift-ph	0.61 $\rightarrow$ 1.0	1.0 $\rightarrow$ 1.0
	lift-mh	0.65 $\rightarrow$ 0.98	0.79 $\rightarrow$ 1.0
	can-ph	0.51 $\rightarrow$ 1.0	0.92 $\rightarrow$ 1.0
	can-mh	0.47 $\rightarrow$ 0.95	0.89 $\rightarrow$ 1.0
	square-ph	0.32 $\rightarrow$ 0.55	0.60 $\rightarrow$ 0.95
	square-mh	0.40 $\rightarrow$ 0.67	0.58 $\rightarrow$ 0.93
	transport-ph	0.58 $\rightarrow$ 1.0	0.74 $\rightarrow$ 1.0
	transport-mh	0.45 $\rightarrow$ 0.91	0.88 $\rightarrow$ 1.0
Image	pusht-image	0.62 $\rightarrow$ 1.0	0.91 $\rightarrow$ 1.0
	lift-ph	0.41 $\rightarrow$ 1.0	1.0 $\rightarrow$ 1.0
	lift-mh	0.85 $\rightarrow$ 1.0	0.90 $\rightarrow$ 1.0
	can-ph	0.51 $\rightarrow$ 0.90	0.71 $\rightarrow$ 0.98
	can-mh	0.39 $\rightarrow$ 0.98	0.56 $\rightarrow$ 0.99
	square-ph	0.21 $\rightarrow$ 0.76	0.67 $\rightarrow$ 0.80
	square-mh	0.30 $\rightarrow$ 0.45	0.58 $\rightarrow$ 0.89
	transport-ph	0.42 $\rightarrow$ 0.77	0.70 $\rightarrow$ 0.79
Nav1D	partial	1.10 $\rightarrow$ 3.91	2.69 $\rightarrow$ 4.42
	full	1.32 $\rightarrow$ 5.98	4.61 $\rightarrow$ 6.24
	expert	5.43 $\rightarrow$ 5.80	6.89 $\rightarrow$ 7.06

we introduced an entropy regularization term to counter this distributional narrowing as much as possible. However, this resulted in the average return improvement to decrease from 32.2%  $\rightarrow$  20.3%.

Additionally, with the alignment process under the Nav1D task, we found the coherency score remained relatively stable with repeated passes and iterations. We monitored this value during training to ensure stable learning, tuning the divergence control hyperparameters as needed. However, we did notice large decreases in the coherency score when we performed multiple passes through the cascading DDPM.

Lastly, we experimented with online fine-tuning, enabling interactions with the environment during the alignment process to collect more data points. We also continued training the Q-value function on these samples. We evaluated this inclusion under D4RL benchmark tasks, and we observed a significantly more stable and efficient training stage with no training collapses and notable improvements in the return achieved.

#### 4.4. Results For Policy-based DMC

In Table 3, we evaluate the performance of Diffusion Policy (DP) using two different action selection methods using the DiT architecture (Peebles & Xie, 2023). Similar to our approach for the planning-based DMC, we applied the alignment approach in sequential order and found multiple rounds still to have return improvements. We find overall improvements in return with our proposed alignment process, more so with the expectation action selection models.

In some cases, we found the energy-based action selection approaches such as IDQL are sufficient to achieve perfect success rates, where we still observed that the fine-tuning did affect the narrowness of the posterior, measured by significantly lower entropy between the generated action candidates.

Regarding the coherency score in the Nav1D task, we found that the alignment process did shift the action distribution away from the behavioral policy, more notably in models trained on the partial and full datasets and upon online fine-tuning. This trend was not as starkly observed in the expert dataset, which retained a comparable coherency score from its reference counterpart.

## 5. Conclusion

In this work, we studied four alignment methods – RL, DPO, SFT, and cascading – for reward maximization in diffusion-based control models (DMC). While these alignment methods were applied independently in prior works, we proposed a unification of these fine-tuning processes using a sequential optimization scheme. Our findings were evaluated in both planning-based and policy-based DMC on various control tasks, and we established the empirical utility of using our proposed alignment approach. For future directions, we suggest finding methods of automating the sequential process, avoiding manual progression on the alignment sequence upon convergence or training failures.

## References

- Ajay, A., Du, Y., Gupta, A., Tenenbaum, J. B., Jaakkola, T. S., and Agrawal, P. Is conditional generative modeling all you need for decision making? In *The Eleventh International Conference on Learning Representations*, 2023. URL <https://openreview.net/forum?id=sP1fo2K9DFG>.
- Bai, Y., Jones, A., Ndousse, K., Askell, A., Chen, A., Das-Sarma, N., Drain, D., Fort, S., Ganguli, D., Henighan, T., et al. Training a helpful and harmless assistant with reinforcement learning from human feedback. *arXiv preprint arXiv:2204.05862*, 2022.
- Black, K., Janner, M., Du, Y., Kostrikov, I., and Levine, S. Training diffusion models with reinforcement learning. *arXiv preprint arXiv:2305.13301*, 2023.
- Cao, H., Tan, C., Gao, Z., Xu, Y., Chen, G., Heng, P.-A., and Li, S. Z. A survey on generative diffusion models. *IEEE Transactions on Knowledge and Data Engineering*, 2024.
- Chen, H., Lu, C., Ying, C., Su, H., and Zhu, J. Offline reinforcement learning via high-fidelity generative behavior modeling. *arXiv preprint arXiv:2209.14548*, 2022.
- Chi, C., Xu, Z., Feng, S., Cousineau, E., Du, Y., Burchfiel, B., Tedrake, R., and Song, S. Diffusion policy: Visuomotor policy learning via action diffusion. *The International Journal of Robotics Research*, pp. 02783649241273668, 2023.
- Clark, K., Vicol, P., Swersky, K., and Fleet, D. J. Directly fine-tuning diffusion models on differentiable rewards. *arXiv preprint arXiv:2309.17400*, 2023.
- Dhariwal, P. and Nichol, A. Diffusion models beat gans on image synthesis. *Advances in neural information processing systems*, 34:8780–8794, 2021.
- Dong, Z., Hao, J., Yuan, Y., Ni, F., Wang, Y., Li, P., and Zheng, Y. Diffuserlite: Towards real-time diffusion planning. *arXiv preprint arXiv:2401.15443*, 2024a.
- Dong, Z., Yuan, Y., Hao, J., Ni, F., Ma, Y., Li, P., and Zheng, Y. Cleandiffuser: An easy-to-use modularized library for diffusion models in decision making. *arXiv preprint arXiv:2406.09509*, 2024b. URL <https://arxiv.org/abs/2406.09509>.
- Fan, Y. and Lee, K. Optimizing ddpm sampling with shortcut fine-tuning. *arXiv preprint arXiv:2301.13362*, 2023.
- Florence, P., Lynch, C., Zeng, A., Ramirez, O. A., Wahid, A., Downs, L., Wong, A., Lee, J., Mordatch, I., and Tompson, J. Implicit behavioral cloning. In *Conference on Robot Learning*, pp. 158–168. PMLR, 2022.
- Fu, J., Kumar, A., Nachum, O., Tucker, G., and Levine, S. D4rl: Datasets for deep data-driven reinforcement learning. *arXiv preprint arXiv:2004.07219*, 2020.
- Gupta, A., Kumar, V., Lynch, C., Levine, S., and Hausman, K. Relay policy learning: Solving long-horizon tasks via imitation and reinforcement learning, 2019. URL <https://arxiv.org/abs/1910.11956>.
- Haarnoja, T., Zhou, A., Abbeel, P., and Levine, S. Soft actor-critic: Off-policy maximum entropy deep reinforcement learning with a stochastic actor, 2018. URL <https://arxiv.org/abs/1801.01290>.
- Hansen-Estruch, P., Kostrikov, I., Janner, M., Kuba, J. G., and Levine, S. Idql: Implicit q-learning as an actor-critic method with diffusion policies. *arXiv preprint arXiv:2304.10573*, 2023.
- Ho, J. and Salimans, T. Classifier-free diffusion guidance. *arXiv preprint arXiv:2207.12598*, 2022.

- Ho, J., Jain, A., and Abbeel, P. Denoising diffusion probabilistic models, 2020. URL <https://arxiv.org/abs/2006.11239>.
- Ho, J., Saharia, C., Chan, W., Fleet, D. J., Norouzi, M., and Salimans, T. Cascaded diffusion models for high fidelity image generation. *Journal of Machine Learning Research*, 23(47):1–33, 2022.
- Hu, E. J., Shen, Y., Wallis, P., Allen-Zhu, Z., Li, Y., Wang, S., Wang, L., and Chen, W. Lora: Low-rank adaptation of large language models. *arXiv preprint arXiv:2106.09685*, 2021.
- Janner, M., Du, Y., Tenenbaum, J. B., and Levine, S. Planning with diffusion for flexible behavior synthesis. *arXiv preprint arXiv:2205.09991*, 2022.
- Kingma, D., Salimans, T., Poole, B., and Ho, J. Variational diffusion models. *Advances in neural information processing systems*, 34:21696–21707, 2021.
- Lipman, Y., Chen, R. T. Q., Ben-Hamu, H., Nickel, M., and Le, M. Flow matching for generative modeling, 2023. URL <https://arxiv.org/abs/2210.02747>.
- Liu, X., Gong, C., and Liu, Q. Flow straight and fast: Learning to generate and transfer data with rectified flow. *arXiv preprint arXiv:2209.03003*, 2022.
- Lu, C., Ball, P., Teh, Y. W., and Parker-Holder, J. Synthetic experience replay. *Advances in Neural Information Processing Systems*, 36, 2024.
- Lugmayr, A., Danelljan, M., Romero, A., Yu, F., Timofte, R., and Van Gool, L. Repaint: Inpainting using denoising diffusion probabilistic models. In *Proceedings of the IEEE/CVF conference on computer vision and pattern recognition*, pp. 11461–11471, 2022.
- Mandlekar, A., Xu, D., Wong, J., Nasiriany, S., Wang, C., Kulkarni, R., Fei-Fei, L., Savarese, S., Zhu, Y., and Martín-Martín, R. What matters in learning from offline human demonstrations for robot manipulation. *arXiv preprint arXiv:2108.03298*, 2021.
- Nichol, A. Q. and Dhariwal, P. Improved denoising diffusion probabilistic models. In *International conference on machine learning*, pp. 8162–8171. PMLR, 2021.
- Ouyang, L., Wu, J., Jiang, X., Almeida, D., Wainwright, C., Mishkin, P., Zhang, C., Agarwal, S., Slama, K., Ray, A., et al. Training language models to follow instructions with human feedback. *Advances in neural information processing systems*, 35:27730–27744, 2022a.
- Ouyang, L., Wu, J., Jiang, X., Almeida, D., Wainwright, C. L., Mishkin, P., Zhang, C., Agarwal, S., Slama, K., Ray, A., Schulman, J., Hilton, J., Kelton, F., Miller, L., Simens, M., Askell, A., Welinder, P., Christiano, P., Leike, J., and Lowe, R. Training language models to follow instructions with human feedback, 2022b. URL <https://arxiv.org/abs/2203.02155>.
- Peebles, W. and Xie, S. Scalable diffusion models with transformers. In *Proceedings of the IEEE/CVF International Conference on Computer Vision*, pp. 4195–4205, 2023.
- Prabhudesai, M., Goyal, A., Pathak, D., and Fragkiadaki, K. Aligning text-to-image diffusion models with reward backpropagation. *arXiv preprint arXiv:2310.03739*, 2023.
- Rafailov, R., Sharma, A., Mitchell, E., Manning, C. D., Ermon, S., and Finn, C. Direct preference optimization: Your language model is secretly a reward model. *Advances in Neural Information Processing Systems*, 36, 2024.
- Ren, A. Z., Lidard, J., Ankile, L. L., Simeonov, A., Agrawal, P., Majumdar, A., Burchfiel, B., Dai, H., and Simchowitz, M. Diffusion policy optimization. *arXiv preprint arXiv:2409.00588*, 2024.
- Rigter, M., Yamada, J., and Posner, I. World models via policy-guided trajectory diffusion. *arXiv preprint arXiv:2312.08533*, 2023.
- Rombach, R., Blattmann, A., Lorenz, D., Esser, P., and Ommer, B. High-resolution image synthesis with latent diffusion models. In *Proceedings of the IEEE/CVF conference on computer vision and pattern recognition*, pp. 10684–10695, 2022.
- Salimans, T. and Ho, J. Progressive distillation for fast sampling of diffusion models. *arXiv preprint arXiv:2202.00512*, 2022.
- Schulman, J., Wolski, F., Dhariwal, P., Radford, A., and Klimov, O. Proximal policy optimization algorithms. *arXiv preprint arXiv:1707.06347*, 2017.
- Silver, D., Lever, G., Heess, N., Degris, T., Wierstra, D., and Riedmiller, M. Deterministic policy gradient algorithms. In *International conference on machine learning*, pp. 387–395. Pmlr, 2014.
- Sohl-Dickstein, J., Weiss, E., Maheswaranathan, N., and Ganguli, S. Deep unsupervised learning using nonequilibrium thermodynamics. In *International conference on machine learning*, pp. 2256–2265. PMLR, 2015.
- Song, J., Meng, C., and Ermon, S. Denoising diffusion implicit models. *arXiv preprint arXiv:2010.02502*, 2020a.

- Song, Y., Sohl-Dickstein, J., Kingma, D. P., Kumar, A., Ermon, S., and Poole, B. Score-based generative modeling through stochastic differential equations. *arXiv preprint arXiv:2011.13456*, 2020b.
- Wallace, B., Dang, M., Rafailov, R., Zhou, L., Lou, A., Purushwalkam, S., Ermon, S., Xiong, C., Joty, S., and Naik, N. Diffusion model alignment using direct preference optimization. In *Proceedings of the IEEE/CVF Conference on Computer Vision and Pattern Recognition*, pp. 8228–8238, 2024.
- Wang, F.-Y., Yang, L., Huang, Z., Wang, M., and Li, H. Rectified diffusion: Straightness is not your need in rectified flow. *arXiv preprint arXiv:2410.07303*, 2024.
- Wang, Z., Hunt, J. J., and Zhou, M. Diffusion policies as an expressive policy class for offline reinforcement learning. *arXiv preprint arXiv:2208.06193*, 2022.
- Williams, R. J. Simple statistical gradient-following algorithms for connectionist reinforcement learning. *Machine learning*, 8:229–256, 1992.
- Xiao, W., Wang, Z., Gan, L., Zhao, S., He, W., Tuan, L. A., Chen, L., Jiang, H., Zhao, Z., and Wu, F. A comprehensive survey of direct preference optimization: Datasets, theories, variants, and applications, 2024. URL <https://arxiv.org/abs/2410.15595>.
- Yang, L., Zhang, Z., Song, Y., Hong, S., Xu, R., Zhao, Y., Zhang, W., Cui, B., and Yang, M.-H. Diffusion models: A comprehensive survey of methods and applications, 2024. URL <https://arxiv.org/abs/2209.00796>.
- Yu, T., Quillen, D., He, Z., Julian, R., Narayan, A., Shively, H., Bellathur, A., Hausman, K., Finn, C., and Levine, S. Meta-world: A benchmark and evaluation for multi-task and meta reinforcement learning, 2021. URL <https://arxiv.org/abs/1910.10897>.
- Zhang, Z., Sun, Y., Ye, J., Liu, T.-S., Zhang, J., and Yu, Y. Flow to better: Offline preference-based reinforcement learning via preferred trajectory generation. In *The Twelfth International Conference on Learning Representations*, 2024. URL <https://openreview.net/forum?id=EG68RSznLT>.
- Zhu, Z., Zhao, H., He, H., Zhong, Y., Zhang, S., Guo, H., Chen, T., and Zhang, W. Diffusion models for reinforcement learning: A survey, 2024. URL <https://arxiv.org/abs/2311.01223>.
- Ziegler, D. M., Stiennon, N., Wu, J., Brown, T. B., Radford, A., Amodei, D., Christiano, P., and Irving, G. Fine-tuning language models from human preferences. *arXiv preprint arXiv:1909.08593*, 2019.